

This article was downloaded by:

On: 23 January 2011

Access details: *Access Details: Free Access*

Publisher *Taylor & Francis*

Informa Ltd Registered in England and Wales Registered Number: 1072954 Registered office: Mortimer House, 37-41 Mortimer Street, London W1T 3JH, UK



## Journal of Coordination Chemistry

Publication details, including instructions for authors and subscription information:

<http://www.informaworld.com/smpp/title~content=t713455674>

### Synthesis, structures and polyphenol oxidase activities of dicopper and dicobalt complexes

Yong Zhang<sup>ab</sup>; Xiang Gao Meng<sup>a</sup>; Zhan Ru Liao<sup>a</sup>; Dong Feng Li<sup>a</sup>; Chang Lin Liu<sup>a</sup>

<sup>a</sup> Key Laboratory of Pesticide & Chemical Biology, Ministry of Education, College of Chemistry, Central China Normal University, Wuhan 430079, P.R. China <sup>b</sup> School of Chemical and Materials Engineering, Huangshi Institute of Technology, Huangshi 435003, P.R. China

**To cite this Article** Zhang, Yong , Meng, Xiang Gao , Liao, Zhan Ru , Li, Dong Feng and Liu, Chang Lin(2009) 'Synthesis, structures and polyphenol oxidase activities of dicopper and dicobalt complexes', *Journal of Coordination Chemistry*, 62: 6, 876 – 885

**To link to this Article:** DOI: 10.1080/00958970802389755

**URL:** <http://dx.doi.org/10.1080/00958970802389755>

PLEASE SCROLL DOWN FOR ARTICLE

Full terms and conditions of use: <http://www.informaworld.com/terms-and-conditions-of-access.pdf>

This article may be used for research, teaching and private study purposes. Any substantial or systematic reproduction, re-distribution, re-selling, loan or sub-licensing, systematic supply or distribution in any form to anyone is expressly forbidden.

The publisher does not give any warranty express or implied or make any representation that the contents will be complete or accurate or up to date. The accuracy of any instructions, formulae and drug doses should be independently verified with primary sources. The publisher shall not be liable for any loss, actions, claims, proceedings, demand or costs or damages whatsoever or howsoever caused arising directly or indirectly in connection with or arising out of the use of this material.

## Synthesis, structures and polyphenol oxidase activities of dicopper and dicobalt complexes

YONG ZHANG<sup>†‡</sup>, XIANG GAO MENG<sup>†</sup>, ZHAN RU LIAO<sup>\*†</sup>,  
DONG FENG LI<sup>†</sup> and CHANG LIN LIU<sup>†</sup>

<sup>†</sup>Key Laboratory of Pesticide & Chemical Biology, Ministry of Education, College of Chemistry, Central China Normal University, Wuhan 430079, P.R. China

<sup>‡</sup>School of Chemical and Materials Engineering, Huangshi Institute of Technology, Huangshi 435003, P.R. China

(Received 10 April 2008; in final form 18 June 2008)

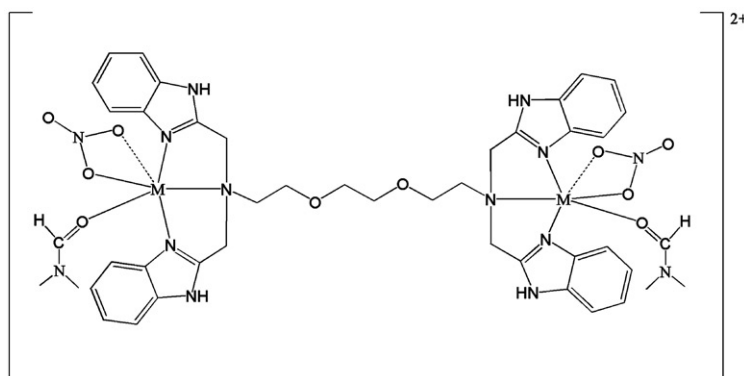
Two dinuclear complexes  $[M_2(EGTB)(NO_3)_2(DMF)_2](NO_3)_2 \cdot 2DMF$  ( $M = Cu$ , **1**;  $Co$ , **2**) were synthesized and structurally characterized, EGTB is *N,N,N',N'*-tetrakis (2-benzimidazolylmethyl)-1,4-diethylene amino glycol ether, and DMF is dimethylformamide. The polyphenol oxidase (PPO) activities of **1** and **2** on pyrogallol oxidation have been investigated, showing that the rate constants  $k_{cat}$  increase with increases of reaction temperatures and pH.

**Keywords:** Dinuclear complexes; Crystal structure; Pyrogallol oxidation; PPO activity

### 1. Introduction

Polyphenol oxidases (PPOs, EC 1.10.3.1) can be divided into type-3 copper proteins containing coupled binuclear copper centers and mononuclear nonheme iron enzymes. They include tyrosinase, catechol oxidase, laccase etc. [1]. Tyrosinases are bifunctional enzymes which catalyze hydroxylation of monophenols to *o*-diphenols and their subsequent oxidation to *o*-quinones, while catechol oxidases catalyze only the latter reaction. Laccase is an oxygen reductase and reacts preferentially with *p*-diphenol [2, 3]. PPOs play a vital role in biological catalytic processes such as animal pigmentation, browning of fruits and vegetables, and lignin biosynthesis of plants. Moreover, polyphenol oxidation is widely applied to medical diagnosis, food refreshment and agricultural cultivation against insects and microbial pathogens [4–6]. In recent years, PPO model complexes have been extensively studied with respect to their structures, kinetics and mechanisms [7–9]. Complexes containing benzimidazole-rich ligands have attracted our interest for a while. Herein, to continue this work, we report the crystal structures and PPO activities of a dicopper(II) and a dicobalt(II) complex coordinated with EGTB (scheme 1).

\*Corresponding author. Email: liaozhanru@yahoo.com.cn



Scheme 1. Chemical structure of the cationic core of dinuclear complex  $[M_2(EGTB)(NO_3)_2(DMF)_2]^{2+}$  ( $M = Cu, 1; Co, 2$ ).

## 2. Experimental

### 2.1. General

All chemicals were purchased from commercial sources and used without further purification. Elemental analyses were obtained using a Perkin–Elmer 2400. Electrospray ionization mass spectra (ESI-MS) in positive ion modes were acquired on an Applied Biosystems API 2000 LC/MS/MS system. UV–Vis spectra were recorded on a Shimadzu UV-265 spectrophotometer. Cyclic voltammetry (CV) was performed with a BAS-100 electrochemical analyzer on a glassy carbon working electrode with a saturated calomel reference electrode and Pt wire serving as the auxiliary electrode. The supporting electrolyte tetrabutylammonium perchlorate (TBAP) was recrystallized twice from methanol.

### 2.2. Preparation of EGTB

Synthesis of EGTB, modified as previously described [10], was obtained by refluxing stoichiometric quantities of ethylene glycol-*bis*-( $\beta$ -aminoethylether)-*N,N,N',N'*-tetraacetic acid (EGTA) and *o*-phenylenediamine (PDA) in glycol at 160–180°C for 6–8 h. The crude product was precipitated by adding distilled water and purified by recrystallization from hot ethanol.

### 2.3. Preparation of $[Cu_2(EGTB)(NO_3)_2(DMF)_2](NO_3)_2 \cdot 2DMF$ (1)

$Cu(NO_3)_2 \cdot 2H_2O$  (0.48 g, 2.0 mmol) was added to DMF solution (10 mL) of EGTB (0.67 g, 1.0 mmol), then stirred at 60°C for 6 h. The dark blue solution was filtered. Blue crystals were obtained by vapor diffusion with anhydrous diethyl ether after seven days. Yield: 60%. Anal. Calcd for  $C_{50}H_{68}Cu_2N_{18}O_{18}$ : C, 44.94; H, 5.09; N, 18.88. Found: C, 44.95; H, 4.90; N, 18.92. IR (KBr,  $cm^{-1}$ ): 3424(m), 1643(s), 1278(s), 424(w), 288(w). Molar conductance,  $\Lambda_m$ : (in DMF solution) 172 S  $cm^2 mol^{-1}$ . UV–Vis spectra [ $\lambda_{max}$ , nm ( $\epsilon$ , L  $mol^{-1} cm^{-1}$ )]: (MeOH solution) 275 (25800).

#### 2.4. Preparation of $[\text{Co}_2(\text{EGTB})(\text{NO}_3)_2(\text{DMF})_2](\text{NO}_3)_2 \cdot 2\text{DMF}$ (**2**)

Red crystals were obtained with a similar reaction procedure as described above, but using  $\text{Co}(\text{NO}_3)_2 \cdot 6\text{H}_2\text{O}$  instead of  $\text{Cu}(\text{NO}_3)_2 \cdot 2\text{H}_2\text{O}$ . Yield: 70%. Anal. Calcd for  $\text{C}_{50}\text{H}_{68}\text{Co}_2\text{N}_{18}\text{O}_{18}$ : C, 45.09; H, 5.12; N, 18.99. Found: C, 44.97; H, 5.05; N, 18.83. IR (KBr,  $\text{cm}^{-1}$ ): 3325(m), 1656(s), 1388(s), 434(w), 282(w). Molar conductance,  $\Lambda_m$ : (in DMF solution)  $165 \text{ S cm}^2 \text{ mol}^{-1}$ . UV-Vis spectra [ $\lambda_{\text{max}}$ , nm ( $\epsilon$ ,  $\text{L mol}^{-1} \text{ cm}^{-1}$ ): (MeOH solution) 278 (23700).

#### 2.5. X-ray structure determination

Crystals of **1** and **2** suitable for X-ray diffraction were sealed in thin-walled quartz capillaries and mounted on a Bruker Smart Apex CCD diffractometer equipped with graphite-monochromated Mo-K $\alpha$  radiation ( $\lambda = 0.71073 \text{ \AA}$ ) at 293 K. Preliminary unit cell constants were determined with a set of 45 narrow frame ( $0.3^\circ$  in  $\omega$ ) scans. Data sets consisted of 1286 frames of intensity data collected with a frame width of  $0.3^\circ$  in  $\omega$ , a counting time of 10 s/frame, and a crystal-to-detector distance of 5.0 cm. Their structures were solved by direct methods and multi-scan absorption corrections were applied using the SAINT+ program [11]. The final refinement was performed with SHELXL-97 [12] by full-matrix least-squares methods on  $F^2$  with anisotropic thermal parameters for non-hydrogen atoms. The hydrogen atoms were generated theoretically onto atoms to which they are attached and refined isotropically with fixed thermal factors [ $U_{\text{iso}}(\text{H}) = 1.2U_{\text{eq}}(\text{aromatic, methylene C and imine N atoms})$ ,  $U_{\text{iso}}(\text{H}) = U_{\text{eq}}(\text{methyl C})$ ]. Crystallographic data of the two complexes are listed in table 1 and selected bond lengths and angles are given in table 2.

#### 2.6. Assay of PPO activity

The PPO activity was measured by pyrogallol oxidation in methanol-Tris-HCl buffer solution (Tris is trihydroxymethyl amino methane). For determination of the kinetic parameters of the complexes, the concentration of pyrogallol was varied from  $1.0 \times 10^{-3}$  to  $1.0 \times 10^{-2} \text{ mol L}^{-1}$ , while that of the complexes were kept at  $1.0 \times 10^{-5} \text{ mol L}^{-1}$ . The determined wavelength was chosen at  $\lambda_{\text{max}} = 325 \text{ nm}$  ( $\epsilon = 4000 \text{ L mol}^{-1} \text{ cm}^{-1}$ ). The pH values and temperatures of reaction system changed in the range of 7.60–8.50 and 20–30°C, respectively.

### 3. Results and discussion

#### 3.1. Crystal structures of the complexes

Both complexes crystallized in the triclinic crystal system, space group  $P\bar{1}$  (table 1) with general formula  $[\text{M}_2(\text{EGTB})(\text{NO}_3)_2(\text{DMF})_2](\text{NO}_3)_2 \cdot 2\text{DMF}$  ( $\text{M} = \text{Cu}$ , **1**;  $\text{Co}$ , **2**). The coordination around copper in **1** can be described as distorted square pyramidal with N1/N2/N4/O3 atoms in the base and carbonyl oxygen O2 occupying the vertex (figure 1). In contrast to **1**, the coordination geometry in **2** can be best described as

distorted octahedral (figure 2), in which two benzimidazolyl nitrogens (N2/N4), one oxygen (O3) of  $\text{NO}_3^-$  and one carbonyl oxygen (O2) of DMF are in the equatorial plane, the amino nitrogen (N1) and the other oxygen (O4) of  $\text{NO}_3^-$  occupy two axial positions; these nitrogens and oxygens are facial in the octahedron. Although the two complexes

Table 1. Crystal data and structure refinement for **1** and **2**.

Complex	<b>1</b>	<b>2</b>
Empirical formula	$\text{C}_{50}\text{H}_{68}\text{Cu}_2\text{N}_{18}\text{O}_{18}$	$\text{C}_{50}\text{H}_{68}\text{Co}_2\text{N}_{18}\text{O}_{18}$
Formula weight	1336.30	1327.08
Crystal size ( $\text{mm}^3$ )	$0.20 \times 0.10 \times 0.04$	$0.30 \times 0.20 \times 0.10$
Crystal system	Triclinic	Triclinic
Space group	$P\bar{1}$	$P\bar{1}$
Unit cells and dimensionals ( $\text{\AA}$ , $^\circ$ )		
<i>a</i>	9.722(3)	10.6482(11)
<i>b</i>	12.124(4)	10.8728(11)
<i>c</i>	14.899(5)	14.8249(15)
$\alpha$	78.813(6)	81.326(2)
$\beta$	71.439(6)	85.549(2)
$\gamma$	70.882(8)	65.841(2)
<i>V</i> ( $\text{\AA}^3$ )	1565.1(9)	1547.9(3)
<i>Z</i>	1	1
$D_{\text{Cacl}}$ ( $\text{g cm}^{-3}$ )	1.418	1.424
<i>F</i> (000)	696	692
<i>h, k, l</i> range	−11/11, −14/13, −17/15	−12/12, −12/12, −14/17
$T_{\text{min}}/T_{\text{max}}$	0.9702/0.8626	0.9407/0.8362
$\theta$ range for data collection ( $^\circ$ )	1.79–25.00	2.07–25.00
Reflections collected	7647	9509
Independent reflections	4760 [ $R_{\text{int}} = 0.0807$ ]	5406 [ $R_{\text{int}} = 0.0629$ ]
Data/restraints/parameters	4760/0/401	5406/0/401
Goodness-of-fit on $F^2$	0.747	0.979
Final <i>R</i> indices [ $I > 2\sigma(I)$ ] <sup>a</sup>	$R_1 = 0.0757$ , $wR_2 = 0.1133$	$R_1 = 0.0560$ , $wR_2 = 0.1412$
<i>R</i> indices [all data]	$R_1 = 0.1844$ , $wR_2 = 0.1542$	$R_1 = 0.0811$ , $wR_2 = 0.1628$
Largest diff. peak and hole ( $\text{e \AA}^{-3}$ )	0.347 and −0.278	0.858 and −0.394

$$^a R_1 = \sum \|F_o\| - |F_c| / \sum |F_o|; wR_2 = [\sum w(F_o^2 - F_c^2)^2 / \sum w(F_o^2)^2]^{1/2}.$$

Table 2. Selected bond lengths ( $\text{\AA}$ ) and angles ( $^\circ$ ) for **1** and **2**.

<b>1</b>		<b>2</b>	
Cu(1)–N(3)	1.923(6)	Co(1)–N(3)	2.043(3)
Cu(1)–N(5)	1.949(6)	Co(1)–N(1)	2.297(3)
Cu(1)–N(1)	2.125(6)	Co(1)–N(4)	2.057(3)
Cu(1)–O(2)	1.987(5)	Co(1)–O(5)	2.075(3)
Cu(1)–O(3)	2.740(2)	Co(1)–O(2)	2.128(3)
Cu(1)–O(5)	2.228(6)	Co(1)–O(3)	2.260(3)
N(3)–Cu(1)–N(5)	159.2(3)	N(3)–Co(1)–N(4)	104.49(12)
N(3)–Cu(1)–O(2)	95.8(2)	N(3)–Co(1)–O(5)	91.25(12)
N(5)–Cu(1)–O(2)	98.1(2)	N(4)–Co(1)–O(5)	154.06(12)
N(3)–Cu(1)–N(1)	82.5(2)	N(3)–Co(1)–O(2)	103.93(12)
N(5)–Cu(1)–N(1)	81.7(2)	N(4)–Co(1)–O(2)	97.56(11)
O(2)–Cu(1)–N(1)	172.3(3)	O(5)–Co(1)–O(2)	98.48(11)
N(3)–Cu(1)–O(5)	101.2(2)	N(3)–Co(1)–O(3)	160.84(12)
N(5)–Cu(1)–O(5)	95.2(2)	N(4)–Co(1)–O(3)	87.00(12)
N(1)–Cu(1)–O(5)	102.2(2)	O(5)–Co(1)–O(3)	84.08(12)
N(5)–Cu(1)–O(3)	95.2(3)	N(4)–Co(1)–N(1)	78.76(10)
O(5)–Cu(1)–O(3)	135.8(2)	O(5)–Co(1)–N(1)	84.51(10)
N(1)–Cu(1)–O(3)	121.9(2)	O(2)–Co(1)–N(1)	176.08(10)

are similar in several aspects, e.g. space group and formula, in the coordination sphere the M–X bonds (M = metal and X = N or O) in **1** are all shorter by more than 0.1 Å than those in **2** except for the M–O<sub>carbonyl</sub> bonds [2.223(2) Å in **1** and 2.075(2) Å in **2**]. The Cu(II) benzimidazolyl nitrogen distances [average 1.938(2) Å] are similar to Cu<sub>2</sub>(NMEDTB)(NO<sub>3</sub>)<sub>3</sub><sup>+</sup> (NMEDTB = *N,N,N',N'*-tetrakis[1-methyl-2-benzimidazolyl]-methyl]-1,2-ethanediamine) [10]. The two Cu(II) ions of **1** are separated by 11.391 Å, which is much longer than the Cu···Cu distance [5.171(2) Å] of Cu<sub>2</sub>(NMEDTB)(NO<sub>3</sub>)<sub>3</sub><sup>+</sup> and too long to have dinuclear coupling in comparison with the Cu···Cu distance 2.9 Å of the natural catechol oxidase isolated from sweet potatoes [13]. Therefore, **1** is best considered as two mononuclear cores.

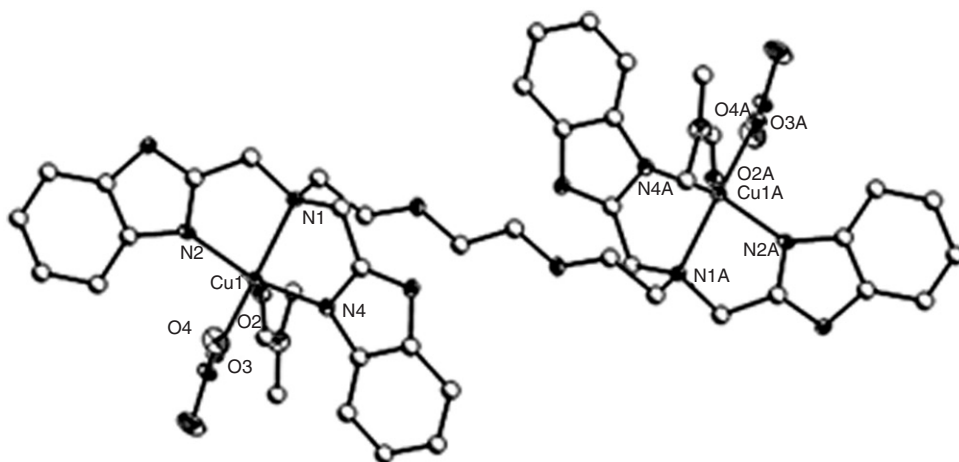


Figure 1. An ORTEP view of the structure of **1**. The hydrogen atoms, non-coordinating NO<sub>3</sub><sup>-</sup> and solvated DMF are omitted for clarity. Symmetry code:  $A = 2 - x, 2 - y, 2 - z$ .

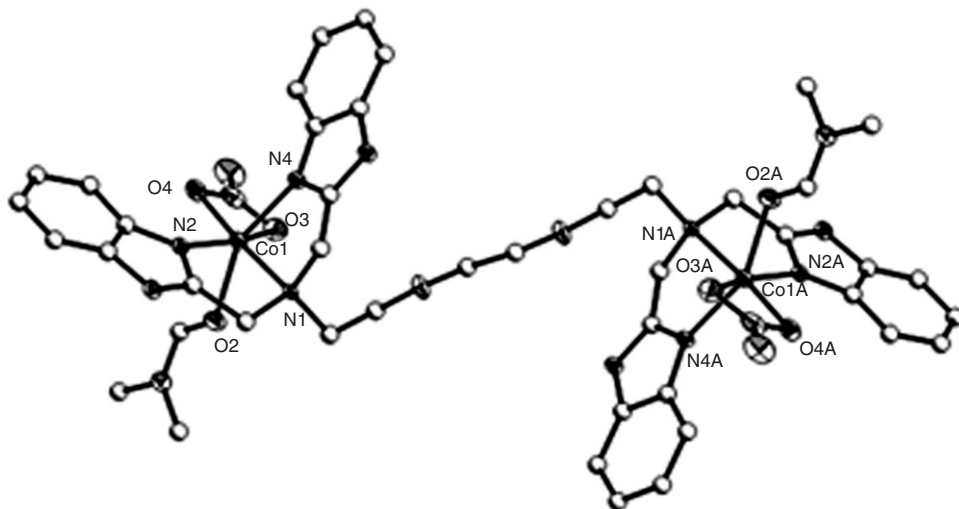


Figure 2. An ORTEP view of the structure of **2**. The hydrogen atoms, non-coordinating NO<sub>3</sub><sup>-</sup> and solvated DMF are omitted for clarity. Symmetry code:  $A = 1 - x, 2 - y, 2 - z$ .

In the molecule structure of **2**, the Co–N(amino) bond is the longest, and the next is Co–O(3) ( $\text{NO}_3^-$ ). The Cu(1)–O3 and Cu1–O4 bond lengths of nitrate of **1** are unequal [1.988(2) Å/2.740(2) Å], but the Co1–O3 and Co1–O4 bonds in **2** are nearly equal [2.128(2) Å/2.260(2) Å]. The reasons underlying these significant alterations in the inner spheres of the metal ions might be the presence of inter- and intra-molecular contacts mediated by the coordinated DMF molecules. The Co...Co distance is 11.804 Å, slightly longer than that of **1**.

### 3.2. Cyclic voltammetry

The redox potential is an important parameter both in electron transfer and catalytic process. The potentials for the two complexes were measured by cyclic voltammetry in the range  $-1.2$  to  $+1.2$  V versus SCE at a scan rate of  $100 \text{ mV s}^{-1}$ . Complex **1** shows a quasi-reversible redox process (figure 3). The cathodic and anodic peak potentials are  $-0.117$  and  $0.050$  V, and the corresponding peak currents are  $1.086 \times 10^{-5}$  and  $7.463 \times 10^{-6}$  A, respectively, which are assigned to a two-electron process  $\text{Cu}_2^{\text{II}} \leftrightarrow \text{Cu}_2^{\text{I}}$ . In comparison with  $E = -0.30$  V versus SCE for pyrogallol, **1** has higher anodic potential, indicating it can oxidize pyrogallol [14]. The redox processes of **2** are irreversible, an anodic peak at  $0.957$  V is assigned to the oxidative peak of  $\text{Co}^{\text{II}} \rightarrow \text{Co}^{\text{III}}$ .

### 3.3. Electrospray ionization mass spectrometry

To track the oxidative products of pyrogallol and further understand the reaction mechanism, electrospray ionization mass spectrometry in positive mode was performed. Pyrogallol was first bound to a metal center to form pyrogallol semiquinone, then oxidized to purpurogallin and a series of their phenol-quinone tautomers [15]. The formation of purpurogallinoid ( $m/z$  104) and formaldehyde ( $m/z$  30) has been reported [16]. From ESI-MS (+) of **1** (figure 4), there seems to exist intradiol and extradiol mechanisms of pyrogallol dioxygenation [17, 18]. The peaks at  $m/z$  57.1, 74.2, 87.1 may

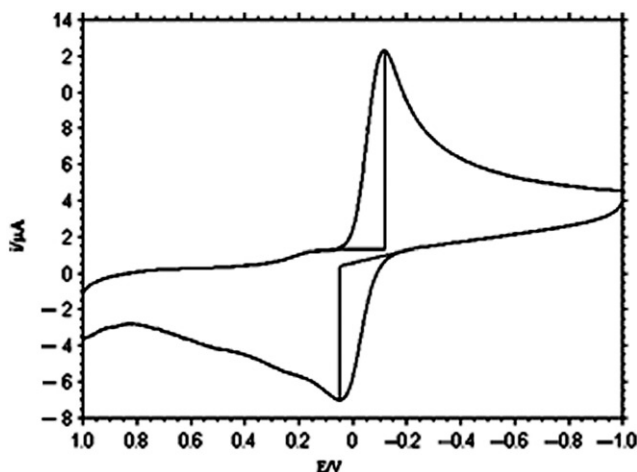


Figure 3. Cyclic voltammogram of **1** in DMF.

be products of McLafferty rearrangement of muconic acid and its dimethyl derivatives [19]. ESI-MS of pyrogallol oxidative products catalyzed by **2** are the same as with **1**. The catalytic reactions seem to be similar.

### 3.4. The PPO activity of the complexes

The kinetic studies of pyrogallol oxidation catalyzed by the two complexes were carried out by the initial velocity ( $V_i$ ) method. When varied concentrations of substrate (pyrogallol, S) was varied and other factors unchanged,  $V_i$  was found to be linear independent on low pyrogallol concentrations. However, at higher pyrogallol concentrations, the catalyst (model complex, M) is saturated and  $V_i$  follows saturation kinetics, namely,  $V_i$  is zero-order with respect to substrate concentrations [S], and the maximum velocity ( $V_{max}$ ) is also obtained at the same time. So a treatment on the basis of Michaelis-Menten model, originally developed for enzyme kinetics, can be applied. Several kinetic parameters  $V_{max}$ ,  $K_m$ ,  $k_{cat}$  and  $k_{cat}/K_m$  were obtained under different conditions (table 3). Here,  $K_m$  is Michaelis constant,  $k_{cat}$  is the turnover number, namely, the amounts (mole) of substrate converted to product per minute per mole of mimetic enzyme. Figure 5 shows  $1/V$  is linear with  $1/[S]$  for **1**, implying

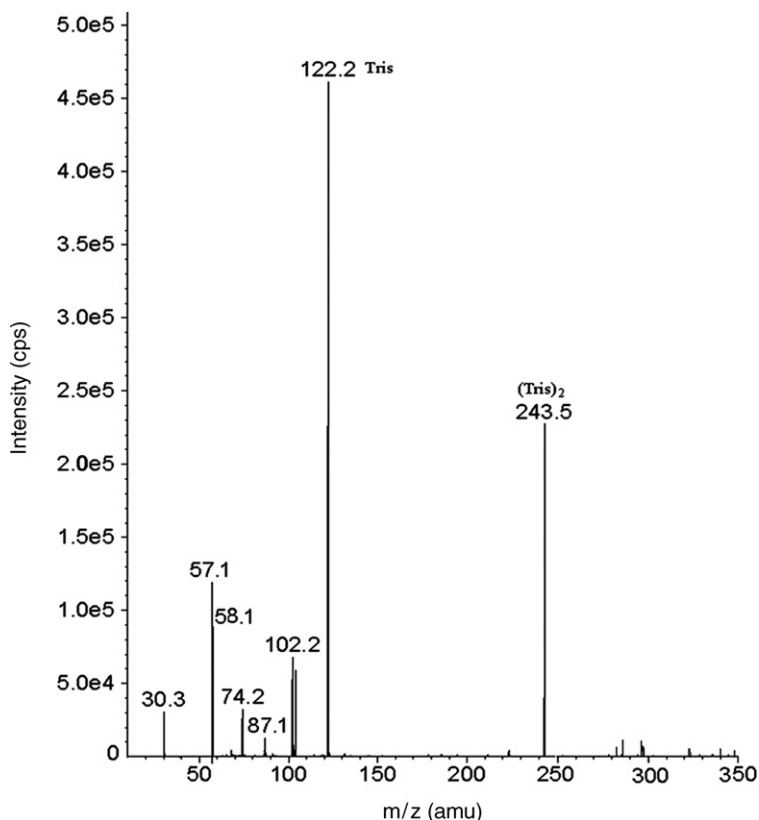
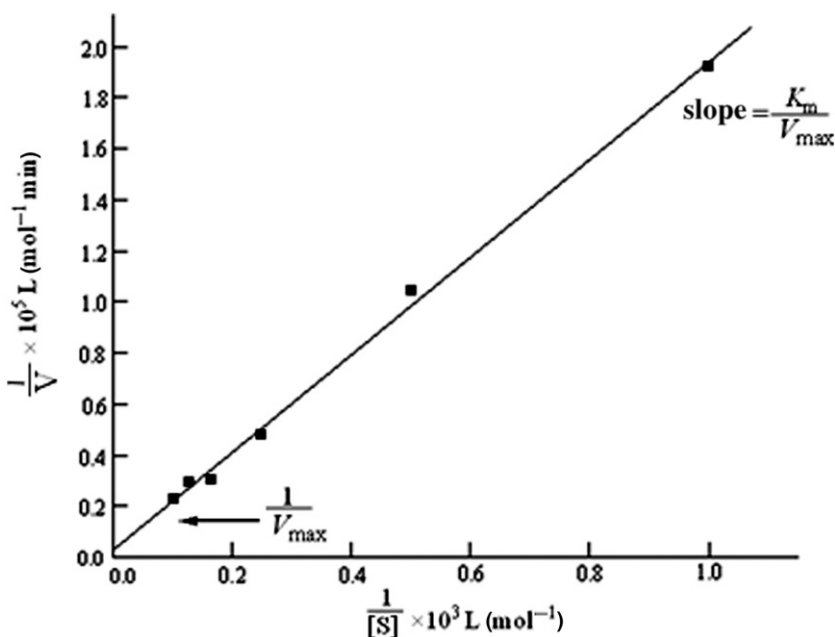


Figure 4. ESI-MS(+) of pyrogallol oxidation catalyzed by **1** in Tris buffer methanol solution (pH 8.00).



Table 3. The kinetic data of two complexes.

Complex	$T$ (°C)	pH	$10^4 V_{\max}$ (mol L <sup>-1</sup> min <sup>-1</sup> )	$10^3 K_m$ (mol L <sup>-1</sup> )	$k_{\text{cat}}$ (min <sup>-1</sup> )	$k_{\text{cat}}/K_m$ (mol L <sup>-1</sup> min <sup>-1</sup> )
Blank	30	8.00	0.02			
<b>1</b>	20	8.00	1.25	2.12	12.50	5.90
	258.00	1.73	2.73	17.30	6.35	
	30	7.60	0.48	1.22	4.80	3.93
	308.00	2.28	3.37	22.8	6.77	
	308.50	3.03	4.01	30.30	7.56	
<b>2</b>	20	8.00	1.16	21.23	11.60	0.55
	258.00	1.25	22.05	12.50	0.57	
	30	7.60	0.23	20.41	2.30	0.11
	308.00	1.86	32.12	18.60	0.58	
	308.50	2.41	34.75	24.10	0.69	

Figure 5. Lineweaver-Burk plot for pyrogallol oxidation catalyzed by **2** at pH 8.00 and 30°C.

a first-order dependence. The slope of the straight line is  $K_m/V_{\max}$ , and the intercept on the vertical axis is  $1/V_{\max}$ .

The results in table 3 are evaluated from Lineweaver-Burk plots. Rate constants increase with increases of reaction temperature and pH of the reaction solution. Moreover,  $k_{\text{cat}}$  of **1** is slightly greater than that of **2**, but the Michaelis constant  $K_m$  of **1** is about 8–16 times lower than that of **2** under the same conditions. Thus, the affinity of **1** for pyrogallol is better, and the formation rate of quinone is slightly faster than for **2**. The difference of the catalytic activities may result from the oxidation state and coordination environment of the complexes. Potentials of PPO model compounds close

to 0 V have excellent activity, while those deviated from the potential 0.2–0.3 V lead to loss of activity partially or completely [20]. The redox potential of **1** is close to 0 V, indicating that the Cu(II)-complex are easily reduced to its Cu(I) after accepting electron from the substrate. But in **2**, the Co(II) ion is difficult to reduce during pyrogallol oxidation. Moreover, coordination around each copper in **1** can be described as distorted square pyramidal, and DMF may be easier to be substituted in the reaction, producing one or two vacant sites to combine with pyrogallol and pyrogallol semiquinone. Compared to the dinuclear distances (3–4 Å) of the typical PPO model compounds described in the literature, the dinuclear distances of the two complexes are too long to bind cooperatively with substrate molecules [21–23]. The PPO activities may be dependent upon the interaction between each active center and substrate.

### Supplementary material

Crystallographic data of the two complexes have been deposited with the Cambridge Crystallographic Data Center as supplementary publication CCDC-283305 (**1**) and CCDC-283372 (**2**). Copies of the data are available from CCDC, 12 Union Road, Cambridge, CB2 1EZ, UK (Fax: +44-1223-336033; Email: deposit@ccdc.cam.ac.uk or www: <http://www.ccdc.cam.ac.uk>).

### Acknowledgement

We thank Key Fundamental Project of China (2002CCA00500) for financial support.

### References

- [1] C. Eicken, B. Krebs, J.C. Sacchettini. *Curr. Opin. Struc. Biol.*, **9**, 677 (1999).
- [2] S. Dieter, S. Willibald. *Angew. Chem.*, **40**, 3791 (2001).
- [3] I.A. Koval, P. Gamez, C. Belle, K. Selmezi, J. Reedijk. *Chem. Soc. Rev.*, **35**, 814 (2006).
- [4] G. Protá. *Med. Res. Rev.*, **8**, 525 (1988).
- [5] G.N. Pruidze, N.I. Mchedlishvili, N.T. Omiadze. *Food Res. Int.*, **36**, 587 (2003).
- [6] C.E. Hall, D. Datta, E.A.H. Hall. *Anal. Chim. Acta*, **323**, 87 (1996).
- [7] A. Neves, L.M. Rossi, A.J. Bortoluzzi, B. Szpoganicz, C. Wiezbicki, E. Schwingel. *Inorg. Chem.*, **41**, 1788 (2002).
- [8] H.C. Liang, M. Dahan, K.D. Karlin. *Curr. Opin. Chem. Biol.*, **3**, 168 (1999).
- [9] E.A. Lewis, W.B. Tolman. *Chem. Rev.*, **104**, 1047 (2004).
- [10] H.M.J. Hendriks, J.M.W.L. Birker, J.V. Rijn. *J. Am. Chem. Soc.*, **104**, 3607 (1982).
- [11] G.M. Sheldrick. SHELSX-97, *Program for the Solution of Crystal Structures*, University of Göttingen, Germany (1997).
- [12] G.M. Sheldrick. SHELXL-97, *Program for the Refinement of Crystal Structures*, University of Göttingen, Germany (1997).
- [13] T. Klabunde, C. Eicken. *Nat. Struct. Biol.*, **5**, 1084 (1998).
- [14] C.J. Doona, K. Kustin. *Int. J. Chem. Kinet.*, **25**, 239 (1993).
- [15] Y. Saeki, M. Nozaki, S. Senoh. *J. Biol. Chem.*, **255**, 8465 (1980).
- [16] Z.F. Chen, Z.R. Liao, D.F. Li, W.K. Li, X.G. Meng. *J. Inorg. Biochem.*, **98**, 1315 (2004).
- [17] M. Velusamy, R. Mayilmurugan, M. Palaniandavar. *J. Inorg. Biochem.*, **99**, 1032 (2005).
- [18] M. Takayama. *Int. J. Mass Spec. Ion Proc.*, **144**, 199 (1995).

- [19] H. Kosugi, K. Kikugawa. *Free Radic. Biol. Med.*, **7**, 205 (1989).
- [20] M.R. Malachowski, H.B. Huynh, L.J. Tomlinson, R.S. Kelly, J.W. Furbeejun. *J. Chem. Soc., Dalton Trans.*, 31 (1995).
- [21] K.D. Karlin, Y. Gultneh, T. Nicholson, J. Zubieta. *Inorg. Chem.*, **24**, 3727 (1985).
- [22] K. Selmezi, M. Réglie, M. Giorgi, G. Speier. *Coord. Chem. Rev.*, **245**, 191 (2003).
- [23] M. Luc, M.G. Emile, C.H. Jean. *Anal. Chim. Acta*, **41**, 209 (2000).